Effect of Interfaces on Dielectric Relaxation in La$_{0.35}$Sr$_{0.6}$MnO$_3$–YSZ

Xia Zheng-Cai,[A] *Tang Chao-Qun,*[A] *Zhou Dong-Xiang*[B] *and Yang Jian-Hui* [A]

[A] Department of Physics, Huazhong University of Science & Technology,
Wuhan 430 074, P. R. China.
[B] Department of Electronics, Huazhong University of Science & Technology,
Wuhan 430 074, P. R. China.

Abstract

The perovskite structure material La$_{0.35}$Sr$_{0.6}$MnO$_3$ was sintered in air and the mixed ceramic of La$_{0.35}$Sr$_{0.6}$MnO$_3$ and 8 mol % Y$_2$O$_3$ + ZrO$_2$ with a 1:1 mass rate was also sintered in air, both at 1530 K for 12 hour. The AC complex impedance spectra have been measured and the effect of the interface between La$_{0.35}$Sr$_{0.6}$MnO$_3$ and YSZ on dielectric relaxation properties of La$_{0.35}$Sr$_{0.6}$MnO$_3$ has been investigated. A schematic of diffusion phase formation and the equivalent circuits are proposed for explaining the results. In the complex impedance spectra, the first and second semicircles correspond to the grain-boundary and interface respectively. The results show that the dielectric relaxation properties and structure of the mixed ceramic are different to that of single phase La$_{0.35}$Sr$_{0.6}$MnO$_3$. The interface has an important effect on the electric properties of the mixed ceramic and produces a dielectric relaxation in low frequency.

1. Introduction

The lanthanum manganite perovskite materials and yttria-stabilised zirconia (YSZ) have been used widely as cathode and electrolyte materials respectively in solid oxide fuel cells (SOFC) (Minh 1993). The efficiency and lifetime of SOFC are related to the properties and structure as well as the interface or the phase boundary of the two components. For the SOFC, the interfaces between cathode and electrolyte should be chemically and structurally stable under long-term operation at 1273 K and, moreover, should be sustainable in the fabrication of SOFC by sintering temperatures higher than 1500 K. In order to improve the stabilisation several investigations have been carried out on the two components and various ideas have been proposed (Stevenson *et al*. 1995; Stochniol *et al*. 1995; Taimatsu *et al*. 1992; Wiil *et al*. 1999; Kleveland *et al*. 1999; Gharbage *et al*. 1994; Jing *et al*. 1999). Generally, the products of La$_2$Zr$_2$O$_7$ and SrZrO$_3$ have been found in the phase boundary. The electrical conductivity of both products is significantly lower than that of YSZ and, thus, the formation of interface products will degrade the properties of the SOFC. However, how the interfaces affect the electrical properties of La$_{0.35}$Sr$_{0.6}$MnO$_3$ is not clear. In the present work, an enhanced interface specimen was fabricated in which the two phases have a 1:1 mass rate, and the AC complex impedance spectra were measured for the samples. Results show that the interface effect can be enhanced with the mixed specimens and observed by comparing the impedance spectra of mixed and single specimens.
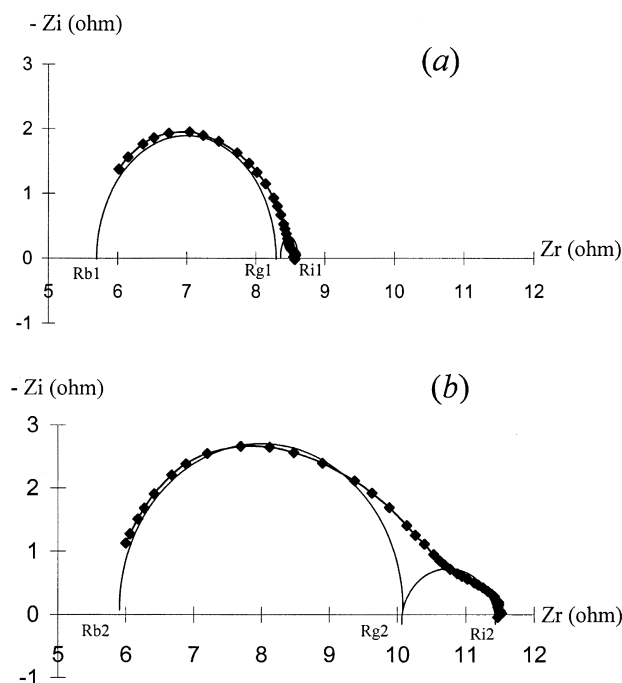
Fig. 1. Impedance spectra for (*a*) LSM6 and (*b*) LSM6–YSZ.

2. Experimental Procedure

The required proportion of starting powders of La_2O_3, $SrCO_3$ and MnO_2 (all of 99.99% purity) were mixed with ethanol and ball-milled for 24 h, followed by drying at 473 K and calcination at 1530 K in air for 12 h. The calcination process was repeated numerous times until the reaction products were confirmed by X-ray diffractometry to be of single-phase, that is perovskite oxide. The compositions of synthesised powder were $La_{0.35}Sr_{0.6}MnO_3$ (also refereed to here as LSM6). In the second step, the powders LSM6 and YSZ with a 1:1 mass rate (LSM6–YSZ) were mixed with ethanol. The mixed powder was ball-milled for 24 h and compacted to flat plates by uniaxial pressing and sintered at 1530 K in air for 12 h. In the same procedure, the LSM6 flat plates were prepared. For impedance spectra measurements, air-drying silver paint was applied on both surfaces of the polished thin plates (diameter 30 mm and thickness 1.5 mm). The complex impedance spectra were measured at room temperature and in the frequency range from 20 Hz to 1 MHz employing HP4284A. The experimental results are shown in Figs 1*a* and 1*b* for the specimens LSM6 and LSM6–YSZ respectively.

   The two impedance spectra can be fitted with two semicircles with different radii and different intersections on the real axis. The values of R_{b1}, R_{g1}, R_{i1}, R_{b2}, R_{g2} and R_{i2} can be calculated from Figs 1*a* and 1*b* and are equal to 5.6, 8.4, 8.6, 5.7, 10.0 and 11.5 Ω respectively. The radii of the two semicircles are equal to 2.8 and 0.2 Ω in Fig. 1*a* and 4.3 and 1.5 Ω in Fig. 1*b*. The two radii of the semicircles for LSM6–YSZ are larger by far than those for LSM6. The differences between the two impedance spectra result from the different structures between LSM6–YSZ and LSM6, especially from the interfaces.

3. Results and Discussion

In polycrystalline electroceramic materials, the grain boundary plays an important role if the boundary is highly conductive or resistive compared to the bulk. On the one hand, such grain boundaries can play a desirable functional role in semiconducting devices such as capacitors. Hence, in many cases, highly resistive grain boundaries are deliberately introduced. On the other hand, the grain boundary conductivity should be as high as possible, such as in SOFC. In the present work, we focus on an investigation of the effects of the grain boundaries of LSM6 and the interfaces between LSM6 and YSZ on the electrical properties of the cathode. In order to enhance the effects of the interface on the electrical properties of LSM6, we fabricated a mixed ceramic of LSM6 and YSZ with a 1:1 mass rate, in which the amount of the interface can be increased. The studies showed that the products of $La_2Zr_2O_7$ and $SrZrO_3$ can be formed in an interface between the lanthanum manganite cathode and YSZ (Wiil *et al*. 1999). From an analysis of the structure, these products have a higher resistivity than the bulk. In order to elucidate the formation of phases of $La_2Zr_2O_7$ and $SrZrO_3$, and the effects of these phases on the cathode electrical properties, the complex impedance spectra can be used. It is well known that the complex impedance spectra allow the separation of impedance contributions from grain interior (bulk) and grain boundaries. Usually, the high-frequency resistance is attributed to the bulk of the polycrystal, whereas the semicircles are assumed to represent the electrical properties of the highly resistive grain boundaries (Kurzweil *et al*. 1989; Van. Dijk *et al*. 1981). For each of the studied samples, a well-defined semicircle should be observed in the complex impedance spectra. Generally, the impedance of the grain interior can be fitted with a resistance and grain boundary with a parallel *R–C* circuit. However, for ceramic specimens, impurity, second phases and defect structure usually segregate in the interface between two ceramic particles. These interfaces contribute to the electric properties and form a new dielectric relaxation. Thus, the second semicircle may be observed in the impedance spectra, as shown in Fig. 1. The equivalent circuits of first and second semicircles for LSM6, corresponding to the grain interior and interface respectively, are shown in Fig. 2*a*.

For single phase LSM6, the electrical properties are mainly attributed to the bulk and grain boundaries. In bulk LSM6, because the radius of the Sr^{2+} ion is different to that of the La^{3+} ion, the lattice distortion around the Sr^{2+} and La^{3+} ions is different as the La^{3+} ions are substituted randomly with Sr^{2+}. Also, the difference in radius between Mn^{3+} (0.65 Å) and Mn^{4+} (0.53 Å) also affects the lattice distortion. The lattice distortion forms a distorted field and obstructs electrons hopping among the Mn-3d states. On the other hand, the charges of Mn^{3+} and Mn^{4+} ions are different which results in different electrostatic fields. Therefore, the Mn ions are localised and trapped by these distorted fields or polarisation fields. When electrons hop from Mn^{3+} to Mn^{4+} via Mn^{3+}–O–Mn^{4+} bonds with activation energy (Goodenough 1955), the distorted fields and electrostatic fields will move together with the hopping. That is, the electrons are localised and trapped by these fields, which result in the formation of bulk resistance. The equivalent circuit of the bulk can be described by R_b, as shown in Fig. 2*a*:

$$R_b = \frac{1}{\sigma_{bulk}} \frac{L}{S} , \tag{1}$$
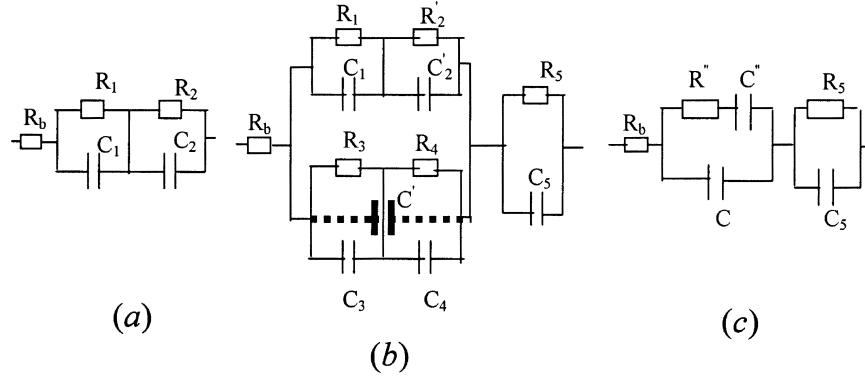
Fig. 2. The equivalent circuits for (*a*) LSM6 and (*b*) LSM6–YSZ, and (*c*) the two series *R*–*C* equivalent circuits.

where L, S and σ_{bulk} are the sample length, electrode area and the conductivity of the bulk. Usually, grain boundaries can be described as a parallel *R*–*C* circuit:

$$R_1 = \frac{1}{\sigma_{gb}} \frac{nL_{gb}}{S},$$ (2)

$$C_1 = \varepsilon_{gb} \frac{S}{nL_{gb}},$$ (3)

where n, L_{gb}, σ_{gb} and ε_{gb} are the number of grain boundary planes parallel to the electrodes, the thickness, conductivity and permittivity of the grain boundaries respectively. In ceramics, the impurity and second phases tend to segregate in interfaces between two neighbour particles. Thus, the scattering of electrons in these interfaces is different from that in the grain boundaries. These interface impurity phases may also affect the dielectric relaxation process and form the second semicircle in the impedance spectra. The interfaces can be described by a plot of R_2–C_2, as shown in Fig. 2a, where

$$R_2 = \frac{1}{\sigma_{in}} \frac{nL_{in}}{S},$$ (4)

$$C_2 = \varepsilon_{in} \frac{S}{nL_{in}},$$ (5)

and where the subscript 'in' denotes the interface.

For LSM6–YSZ, the electrical properties are attributed to the bulk and grain boundaries of LSM6 and YSZ respectively. Additionally, the interface between LSM6 and YSZ also affects the electrical properties due to the segregation of highly resistive products in the interface. However, experiment showed that the impedance spectrum of LSM6–YSZ is similar to that of LSM6, which can be interpreted from the structure of LSM6–YSZ. In LSM6–YSZ, the LSM6 and YSZ have the same particle size and are mixed with a 1:1 mass rate. Thus, the two phases can form linked nets. In the linked LSM6 nets, electrons can be transported in the net, and the mixed LSM6–YSZ should have approximately the same conductivity as the single LSM6. The result can be verified from the impedance
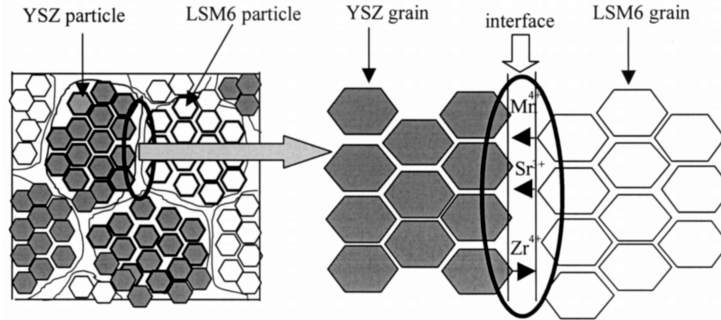
Fig. 3. The interface and ion diffusion between LSM6 and YSZ.

intersection on the real R_{b1} and R_{b2}, where R_{b1} approximately equals R_{b2} and the slight difference in the intersection results from the linked net of LSM6 being locally separated by YSZ. In Fig. 1, the radius of the first semicircle for LSM6–YSZ is larger than that for LSM6, which can be interpreted from the interface diffusion shown in Fig. 3.

In Fig. 3 we have made four assumptions: (1) the YSZ and LSM6 particles are distributed uniformly with the same size, (2) the LSM6 particles form a linked net in which electrons can transport via Mn^{3+}–O–Mn^{4+}, (3) the YSZ particles are electrical insulators, and (4) all LSM6 and YSZ particles have homogeneous electrical properties. At high temperature, the ions La^{3+}(1.22 Å), Mn^{4+}(0.53 Å), Mn^{3+}(0.65 Å), Sr^{2+}(1.27 Å), Zr^{4+}(0.87 Å) and Y^{3+}(1.06 Å) will diffuse to the interfaces and into other particles along the grain boundaries. These diffused ions will form second phases in the interfaces and grain boundaries. Wiil *et al.* (1999) have proposed that the formation of secondary phases at the interface between lanthanum manganite and YSZ in air may be represented by the simplified reactions

$$2ZrO_2 + 2LaMnO_3 = La_2Zr_2O_7 + \tfrac{1}{2}O_2, \tag{6}$$

$$2ZrO_2 + SrMnO_3 = SrZrO_3 + MnO + \tfrac{1}{2}O_2. \tag{7}$$
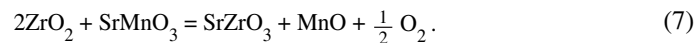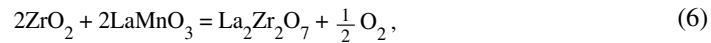
Among the ions, the diffusion coefficients of the Mn^{4+} and Zr^{4+} ions are higher than those of the others because of their smaller ion radii. There is an Mn-deficient layer near the LSM6 due to the diffusion of Mn^{4+} into the interfaces. This Mn deficiency is of benefit to the formation of $La_2Zr_2O_7$ and $SrZrO_3$. Further, the Zr^{4+} ions also have a high diffusion coefficient resulting from its small ion radius. The Zr^{4+} ions will diffuse into LSM6 along the grain boundaries of LSM6. The diffused ions will form second phases, such as $La_2Zr_2O_7$ and $SrZrO_3$, in the grain boundaries of LSM6. Similarly, Mn^{4+} ions will also diffuse into YSZ along the grain boundaries and form $La_2Zr_2O_7$. These segregated second phases have an important effect on the electrical properties of LSM6. Thus, the grain boundary resistivity of LSM6–YSZ will be larger than that of LSM6, and the radius of the second semicircle for LSM6–YSZ should be larger than that for LSM6, a result observed in Fig. 1.

The equivalent circuit of the bulk of the phase LSM6–YSZ can be described by R, and the grain boundaries of LSM6–YSZ, including that of LSM6 and YSZ, can be described

by R_1–C_1, $R_2^{'}$–$C_2^{'}$, R_3–C_3 and R_4–C_4. These resistances and capacitances can be described with the same equations as (1)–(5). Additionally, the high resistive interface between LSM6 and YSZ plays an important role in the electrical properties. At high frequencies, the highly resistive grain boundary of LSM6, the highly resistive interfaces and highly resistive YSZ phases are capacitively conducting. The large interface capacitance, the large grain boundary capacitance and the large YSZ bulk capacitance short the boundary of the LSM6 and YSZ phases for the entire dielectric relaxation of the sample. Thus, it shows purity impedance. Since the impedance of bulk YSZ is very large, the YSZ phases can be regarded approximately as an open circuit. The equivalent circuits of the YSZ phases can be described by the capacitance $C^{'}$, as shown by the dotted line in Fig. 2*b*. Thus, the mixed ceramic LSM6–YSZ can be described as two series R–C equivalent circuits, as in Fig. 2*c*. In the complex impedance spectra, the radius of the first semicircle for LSM6–YSZ is larger than that for LSM6, due to the diffusion of Zr^{4+} ions and the formation of highly resistive $La_2Zr_2O_7$ and $SrZrO_3$.

In the interface between LSM6 and YSZ, the impedance and capacitance can be written as

$$R_5 = \frac{1}{\sigma_{in}} \frac{nL_{in}}{S},\tag{8}$$

$$C_5 = \varepsilon_{in} \frac{S}{nL_{in}},\tag{9}$$

where σ_{in}, ε_{in} and L_{in} are the conductivity, permittivity and the thickness of the interface respectively. Thus, the second semicircle can be observed in complex impedance spectra, corresponding to R_5–C_5, as shown in Fig. 2*c*.

4. Conclusions

The effects of the electrical properties of highly resistive grain boundaries and highly resistive interfaces in the electroceramic can be investigated with complex impedance spectra. For polycrystalline electroceramic materials, the dielectric relaxation was determined mainly by the grain interior and boundaries. For the single phase LSM6, the electrical properties can be described by bulk and grain boundaries, corresponding to the resistance R_b of the first R–C equivalent circuits. The dielectric relaxation is mainly determined by the grain boundary, and the interfaces have only a slight effect on the relaxation.

For the mixed phases LSM6–YSZ, the electrical properties can be described with a resistance and two series R–C equivalent circuits, corresponding to the bulk, the grain boundaries of LSM6, and the interfaces between LSM6 and YSZ respectively. The bulk, grain boundary and interface electrical resistivities of LSM6–YSZ are larger than that of the single phase LSM6 due to the diffusion of ions and the formation of high resistive segregation in the grain boundaries and interfaces. Thus, the effect of the interfaces on dielectric relaxation is enhanced compared to that of the single phase YSZ. The effect will degrade the electrical properties of LSM6 cathode materials.

The sinter temperature and sinter time in the preparation of the samples have a direct effect on the diffusion and formation of high resistance products. In order to improve the performance of solid oxide fuel cells, the interface phases between the lanthanum manganite cathode and the YSZ electrolyte should be restrained, a subject we will investigate in future work.

References

Gharbage, E., Pagnier, T., and Hammou, A. (1994). *J. Electrochem. Soc*. **141**, 2118.

Goodenough, J. B. (1955). *Phys. Rev*. **100**, 564.

Jing, S. P., Love, J. G., and Zhang, J. P. (1999). *Solid State Ionics* **121**, 1.

Kleveland, K., Einarsrud, M. A., and Schmidt, C. R. (1999). *J. Am. Ceram. Soc*. **82**, 729.

Kurzweil, P., Ober, J., and Wabner, D. W. (1989). *Electrochim. Acta* **34**, 1179.

Minh, N. Q. (1993). *J. Am. Ceram. Soc*. **76**, 536.

Stevenson, J. W., Hallman, P. F., and Armstrong, T. R. (1995). *J. Am. Ceram. Soc*. **78**, 507.

Stochniol, G., Syskakis, E., and Naoumidis, A. J. (1995). *Am. Ceram. Soc*. **78**, 929.

Taimatsu, H., Wada, K., and Kaneko, H. (1992). *J. Am. Ceram. Soc*. **75**, 401.

Van Dijk, T., and Burggraff, A. J. (1981). *Phys. Stat. Solidi (a)* **63**, 229.

Wiil, K., Schmidt, C. R., Faaland, S., and Shamsili, S. (1999). *J. Am. Ceram. Soc*. **82,** 721.